Desalination and Water Treatment
www.deswater.com

doi: 10.5004/dwt.2017.21068

91 (2017) 374–385
October

Investigations on the effectiveness of the Saba banana peel for the treatment of fluoride contaminated water

Manisha Poudyal, Sandhya Babel*

School of Biochemical Engineering and Technology, Sirindhorn International Institute of Technology (SIIT), Thammasat University, Pathum Thani, Thailand, Tel. +662 986 9009 Ext. 2307; emails: sandhya@siit.tu.ac.th (S. Babel), poudyal.manisha@gmail.com (M. Poudyal)

Received 19 December 2016; Accepted 20 June 2017

ABSTRACT

This study aims to evaluate the effectiveness of Saba banana peel powder, an agro-based adsorbent for the removal of excess fluoride from water. A series of batch adsorption experiments were carried out to determine the influence of adsorbent dose, pH, agitation speed, contact time, initial fluoride concentration and the effect of co-existing ions (F^-/Cl^- and F^-/SO_4^{2-}). The adsorbent–fluoride interactions were more pronounced at neutral pH, and equilibrium was attained within 160 min, where 82% removal efficiency was recorded for 10 mg/L fluoride solution. FTIR results showed the presence of various functional groups (–OH, $–NH_2$, –COOH), which played a major role in fluoride removal. The fluoride removal rate decreased at a higher concentration of sulfate ions, but was independent of the presence of chloride ions. The experimental data followed pseudo-second-order kinetics and fitted well with both Langmuir and Freundlich isotherms. This implied the predominance of chemisorption process on the heterogeneous surface of adsorbent. The linear relationships with high R^2 values (>0.99) for both isotherms proved that the experimental data were statistically significant. Despite having low surface area (1.87 m^2/g), this abundantly available horticultural waste showed remarkable fluoride adsorption capacity of 5.9 mg/g, and the residual fluoride concentration also met the WHO regulated standard.

Keywords: Fluoride; Saba banana peel; Batch adsorption; Isotherms; Kinetics

1. Introduction

Fluoride (F^-) is the simplest ion of element fluorine and is ubiquitous in all environmental components like air, water, soil and rocks. Its concentration is highly dependent on the proximity to the sources of emission. On a global scale, fluoride originates dominantly from natural processes, and a trace amount is commonly encountered in water sources. Basically, fluoride is released into water bodies as a result of weathering of fluoride bearing minerals or leaching from soil into groundwater under favorable dissolution conditions and percolating water pressure. Calcite and fluorite are two major solubility-control minerals influencing the geochemistry of high fluoride content water. Systemic fluorides, such as community water fluoridation and dietary fluoride supplements are often promoted in order to lessen tooth decay. The optimum level of fluoride (0.5–1 mg/L) in drinking water is beneficial for normal mineralization of teeth and skeletal structures, and helps in the effective reduction of dental decay. However, continued consumption of fluoride containing water (above a threshold of 1.5 ppm) may be associated with negative health effects, such as dental fluorosis, severe skeletal and non-skeletal fluorosis, cardiovascular disease, as well as lowering of IQ [1,2]. Endemic fluorosis has been reported in about 25 developed and developing nations throughout the world.

The WHO recommended value of fluoride in drinking water is 1.5 mg/L, set with a target between 0.8 and 1.2 mg/L to maximize the benefits and offset the harmful effects. In the

* Corresponding author.

Presented at the 13th IWA Specialized Conference on Small Water and Wastewater Systems & 5th IWA Specialized Conference on Resources-Oriented Sanitation, 14–16 September, 2016, Athens, Greece.

absence of alternative water supplies, the only feasible option to prevent fluorosis is to treat the fluoridated water by employing various defluoridation techniques. The Nalgonda technique is a commonly practiced method at the domestic level, which includes an addition of an aluminum salt, lime and bleaching powder, followed by quick mixing, flocculation, sedimentation and filtration. But this process generates a large amount of toxic alum and fluoride sludge. Other sophisticated technologies, such as hybrid precipitation–microfiltration, oxidation–reduction, membrane process like reverse osmosis and ion-exchange resins and electro-chemical processes based on electrolysis, are invariably more costly and not technically feasible, especially in rural areas. Moreover, adsorption by activated alumina, bone char, costly commercial activated carbons and nanoparticles are highly efficient in lowering fluoride concentration to the permissible level. Yet, their uses have been limited in water treatment applications due to social, financial, cultural and environmental reasons [3,4]. All these methods have their inherent merits and demerits.

Amongst the aforementioned methods, adsorption has been recognized as the most desirable one for the removal of fluoride from aqueous medium, as it offers economic feasibility and simplicity in design and operation. In addition, agro-based residues are gaining more attention as they can meet the demand for safe, eco-friendly and abundantly available low-cost adsorbents. A wide range of plant-based materials like cabbage tree seeds [5], canola and sorghum stalks [6], *Vitex negundo* barks [7], pineapple peel [8], mosambi peel [9], *Musa paradisiaca* peel and coffee husk [10] have been investigated as adsorbents for removing fluoride from water. So far, defluoridation of water using Saba banana peels has not been reported anywhere in the literature in spite of their ubiquitous distribution. The annual world production of bananas in about 120 countries is estimated to be over 68 million tons, and in South-East Asia, Thailand ranks third in terms of production. Particularly, Saba bananas are the most widely disseminated ABB cultivar used for cooking in Thailand. These bananas are comparatively cheaper than the plantain and desert bananas. They work extremely well as fritters, chips, sticky sweets, many desserts, banana cue and in many other ways for the street vendors. However, the banana peels are a major horticultural by-product, generated in large quantities and often discarded as solid waste. The peels form about 18%–33% of the whole fruit. If these wastes can be recycled, then a portion of the solid waste problem will be addressed. So, utilizing these zero-cost peels for defluoridation adds value to these wastes while solving a major environmental problem. Banana peels have been used to purify drinking water as they contain a number of molecules capable of removing impurities present in water. The peels are scientifically shown to have both antifungal and antibiotic components. Various literature support that the bioactive compounds like flavonoids, tannins, phlobatannins, alkaloids, glycosides and terpenoids present in the peel might be responsible for the antibacterial activity against microorganisms and periodical pathogens [11].

Taking all these factors into consideration, the present study focuses on the adsorption of fluoride in a batch system by Saba banana peel powder as a novel and cost-effective adsorbent. The knowledge of the optimal conditions would herald a better design and modeling process. Thus, the effect of adsorbent dose, pH, agitation speed, contact time, initial fluoride concentration and effect of major co-existing ions on fluoride removal are evaluated.

2. Materials and methods

2.1. Preparation and characterization of adsorbent

Saba banana peels were collected from the local fruit market in Thailand and were washed thoroughly with tap water to remove the attached fleshy residues. The peels were dried in sunlight for about 7–8 h, followed by drying in a hot air oven at 120°C ± 2°C for 36 h. It is supposed that a higher temperature would expand the surface area of adsorbents and facilitates the interaction between the ligands on the cell wall and the fluoride ions. The dried peels were crushed using a mortar and pestle and sieved by 250 BSS, mesh size. Finally, the screened Saba banana peel (SBP) powder was stored in a sterilized airtight container.

Characterization of adsorbent is important in adsorption studies, as it helps us to understand the adsorbent properties and interaction behaviour with fluoride. The specific surface area of the prepared adsorbent was determined by N_2 gas adsorption/desorption at 77 K using a single-point BET surface area analyzer supplied by MicrotracBEL, Japan, Inc. The measurement was automatically done by Belsorp Adsorption/Desorption Data Analysis Software – Version 6.3.2.0, available within the instrument. In order to obtain the FTIR spectra for functional group analysis, a very small amount of SBP was ground and mixed with spectral-grade KBr in a ratio of 1:10, and pressed under high vacuum pressure to obtain transparent pellets. The FTIR data were collected over 4,000–500 cm^{-1} at 4 cm^{-1} resolution on a Thermo Nicolet 6700 FTIR Spectrometer (Thermo Electron; USA). The simple spectra are obtained from the adsorbent with few IR active covalent bonds. Likewise, for examining the surface morphology of the adsorbent, small fragments of SBP were mounted on a 10 mm aluminum stub with a carbon adhesive and coated with platinum before observation. The morphological features before and after fluoride adsorption were then studied using a 3D real surface view microscope VE-8800 Series (KEYENCE, Japan) under low voltage with variable pressure mode.

2.2. Experimental setup for batch adsorption studies

The stock fluoride solution of 1,000 mg/L was prepared by dissolving 2.21 g AR grade anhydrous sodium fluoride in Milli-Q water. An experimental test solution of 10 mg/L F^- concentration was prepared by serial dilution of fresh stock solution to represent environmentally relevant conditions. A series of batch adsorption experiments were carried out in 250 mL Erlenmeyer flasks, with 50 mL of test solution at room temperature (25°C ± 3°C). The flasks were sealed to prevent changes in solution volume during the experiment, and constantly agitated in an NB-101 M Orbital shaker (N-Biotek Inc., Gyeonggi-Do, Korea). After a predefined time interval, samples were filtered with Whatman No. 42 filter paper, and the residual fluoride concentration was measured using an ExStik FL700 Fluoride meter equipped with an ion-selective electrode (FLIR Systems, USA). This procedure follows the American Society for Testing and Materials and EPA standard methodology, using total ionic strength adjustment buffer reagents. The graphs of fluoride removal were plotted as a function of various operating parameters with the average value of duplicate runs. The error in the experimental data

is ±1%–2% for percentage removal and ±0.005–0.01 mg/g for amount of fluoride adsorbed. The amount of fluoride adsorbed at equilibrium contact time, q_e (mg/g), and the fluoride removal efficiency were calculated using Eqs. (1) and (2):

$$\text{Equilibrium uptake Capacity } \left(q_e\right) = \frac{C_i - C_e}{W} \times V \quad (1)$$

$$\text{Percentage Removal } \left(\%\right) = \frac{C_i - C_e}{C_i} \times 100 \quad (2)$$

where C_i and C_e (mg/L) are the liquid-phase fluoride concentrations at initial and equilibrium time, W is the dry weight of the adsorbent (g) and V is the volume of fluoride solution (L).

2.3. Optimization of operating parameters

The optimum reaction conditions for maximum defluoridation were determined by studying the influence of adsorbent dose, pH, agitation speed, contact time, initial fluoride concentration and effect of co-existing ions in the binary components system. For optimizing a certain parameter, all other variables were kept constant, and only one specific parameter was varied.

2.3.1. Effect of adsorbent dose

The dosage is a crucial parameter as it determines the capacity of adsorbents for a certain fluoride concentration under a given set of operating conditions. The effect of adsorbent dose on the fluoride removal was assessed by varying the amount of SBP from 0.5 to 5 g/L (0.5, 1, 1.5, 2, 2.5, 3, 3.5, 4, 4.5 and 5 g/L) in a 10 mg/L fluoride solution at neutral pH. The mixture was constantly shaken at 150 rpm for 2 h.

2.3.2. Effect of pH

The relationship between pH scale and fluoride removal was studied within the domain of 2–10 by adding drops of 0.1 N HCl or NaOH into the test solution. The optimized dose of SBP was added into the solution and agitated at 150 rpm for 2 h. Finally, the residual fluoride concentration was measured, and the optimum pH value was chosen. The pH of a solution was measured using Hanna digital pH meter. A standard glass-combination electrode pH meter was calibrated against commercial buffer solutions of known pH value.

2.3.3. Effect of agitation speed

The agitation speed plays a vital role in the distribution of solute in the bulk solution and the formation of an external boundary film. The influence of this parameter was monitored at low, medium and high speeds (100, 150, 200, 250 and 300 rpm) under optimized dose and neutral pH, for 2 h of contact time.

2.3.4. Effect of contact time

The kinetics of fluoride uptake was examined as a function of shaking time from 40 to 240 min at an interval of 40 min. A test solution, maintained at neutral pH with optimum adsorbent dose, was shaken at a specified speed for the required time intervals. Then, the optimum residence time was evaluated after the attainment of equilibrium.

2.3.5. Effect of initial fluoride concentration

The adsorbent dose, contact time and pH required to bring the fluoride concentration to the accepted level depends on the initial fluoride concentration. Once all the parameters were optimized for maximum fluoride removal, the effect of initial fluoride concentration was examined by varying the fluoride concentration from 5 to 40 mg/L.

2.3.6. Effect of co-existing ions

In addition to fluoride, the aqueous solution may contain several other anions, such as Cl^-, SO_4^{2-}, CO_3^{2-}, PO_4^{3-}, HCO_3^- and NO_3^- at varying concentrations, which may impede the fluoride removal process. The selective nature of the fluoride by the adsorbent depends on size, charge, polarizability, electro negativity difference, etc. In this study, the concentrations of sulfate and chloride were kept much higher than fluoride, so that the synthetic solution resembles a real groundwater sample. The concentration of each anion was varied from 50 to 250 mg/L in the presence of 10 mg/L fluoride at neutral pH. The fluoride removal efficiency of banana peel adsorbent was evaluated under the optimum reaction conditions.

2.4. Adsorption isotherms

Adsorption isotherms deal with the specific relationship between the equilibrium amount of fluoride on the adsorbent and in solution at constant temperature and pH. For the purpose of design, the experimental data were analyzed with Langmuir and Freundlich models. These models are chosen in this study because of their simplicity, and they can be easily linearized.

2.4.1. Langmuir adsorption isotherm

The Langmuir isotherm assumes monolayer coverage of fluoride ions onto the adsorbent surface having energetically equal homogeneous sites, with no lateral interaction and steric hindrance between the adsorbed molecules [12]. The linear form of the Langmuir isotherm model is expressed mathematically as:

$$\frac{C_e}{q_e} = \frac{1}{Q_{ob}} + \frac{C_e}{Q_o} \quad (3)$$

where q_e and C_e refer to the amount of fluoride adsorbed per unit weight of adsorbent (mg/g) and the equilibrium fluoride concentration in solution (mg/L), respectively; Q_o and b are Langmuir constants related to the maximum adsorption capacity (mg/g) and adsorption affinity coefficient (L/mg), calculated from the slope and intercept of the linear plot of C_e/q_e vs. C_e. The essential features of the Langmuir isotherm were interpreted in terms of the dimensionless constant separation factor, R_L:

$$R_L = \frac{1}{1 + bC_i} \tag{4}$$

where C_i is the initial fluoride concentration (mg/L) and b is the reciprocal of concentration at which half saturation of adsorbent is attained. The R_L value confirms whether the adsorption process is unfavorable ($R_L > 1$), linear ($R_L = 1$), favorable ($0 < R_L < 1$) or irreversible ($R_L = 0$) [13].

2.4.2. Freundlich adsorption isotherm

The Freundlich isotherm describes a multilayer adsorption process on the heterogeneous surface having a non-uniform distribution of heat of sorption [14]. The stronger sites are occupied in the beginning, and then the energy of adsorption decreases exponentially upon completion of the adsorption process. Eq. (5) represents the logarithmic form of the Freundlich isotherm model:

$$\log q_e = \log K + \frac{1}{n} \log\ C_e \tag{5}$$

where C_e and q_e are equilibrium fluoride concentration (mg/L) and adsorption capacity (mg/g), respectively; K and n are the Freundlich constants denoting the adsorption capacity (mg/g) and adsorption intensity, respectively. The logarithmic plot of $\log q_e$ vs. $\log C_e$ should result in a straight line, and the values of these constants can be obtained from the slope and intercept of the respective plot. The computed value of n should lie between 1 and 10 for the adsorption process to be favorable [15].

2.5. Adsorption kinetic models

Kinetic studies are needed to select the residence time of the adsorbent for batch or continuous fluoride removal. The experimental data from the time vs. fluoride removal curves were fitted to three kinetic models, namely the pseudo-first-order, pseudo-second-order and intraparticle diffusion models, to elucidate the sorbent–sorbate interactions with the most probable rate-controlling mechanisms.

2.5.1. Pseudo-first-order kinetic model

The first-order rate equation developed by Lagergren applies best for describing the adsorption of solute based on solid adsorption capacity [16]. It is the earliest known model which intuitively relates to one-site occupancy, directed by surface reaction rate and is expressed as:

$$\log\left(q_e - q_t\right) = \log\ q_e - \frac{K_1}{2.303} t \tag{6}$$

where q_e and q_t (mg/g) are the amount of fluoride adsorbed at equilibrium and time, t (min), and K_1 (min^{-1}) is the pseudo-first-order rate constant. This equation is only applicable when the measured concentration is equal to the surface concentration, and the parameter $K_1 (q_e - q_t)$ does not denote the number of available binding sites. Thus, the reaction rate is limited by only one mechanism, and all the sites are dependent on time. A plot of $\log(q_e - q_t)$ against t should give a linear relationship, from which the values of K_1 and q_e can be computed.

2.5.2. Pseudo-second-order kinetic model

When the pseudo-first-order kinetics equation is not applicable, generalization for a two-site-occupancy adsorption system is proposed, which is known as the pseudo-second-order kinetic equation [17]. The main assumptions for this model is that the two reactions are occurring simultaneously. The first one is fast and reaches equilibrium quickly, while the second one is slower and continues for a longer time covering the entire adsorption process. Pseudo-second-order kinetics is a lump sum parameter of the chemical reaction and the physical diffusion process, and is given as:

$$\frac{t}{q_t} = \frac{1}{h} + \frac{t}{q_e} \tag{7}$$

where $h = K_2 q_e^2$ is defined as the initial adsorption rate (mg g^{-1} min^{-1}), q_e and q_t (mg/g) denote the fluoride uptake at equilibrium and at time t (min), and K_2 is the pseudo-second-order rate constant (g mg^{-1} min^{-1}). The values of the theoretical equilibrium sorption capacity (q_e) and rate constant (K_2) can be obtained from the slope and intercept of the linear plot of $\frac{t}{q_t}$ vs. t.

2.5.3. Intraparticle diffusion model

This model is particularly used to evaluate the significance of a diffusion-controlled process (internal or intraparticle diffusion) on the fluoride removal. Adsorption diffusion models consist of one or more consecutive steps. Therefore, the whole adsorption process may be governed by pore diffusion, surface diffusion, external or film diffusion, internal diffusion or through a combination of these. The Weber–Morris intraparticle diffusion model assumes that the fluoride uptake rate is directly proportional to the square root of contact time ($t^{1/2}$) instead of time, t [7] and is given by the following equation:

$$q_t = k_{\text{int}} t^{1/2} + C \tag{8}$$

where k_{int} is the diffusion coefficient (mg g^{-1} min$^{-0.5}$) obtained from the slope of the graph plotted between q_t and $t^{1/2}$; and C is the intraparticle diffusion constant (mg g^{-1}), related to the boundary layer thickness.

The suitability of the aforementioned equations are judged by the correlation coefficient (R^2) values. According to the regression analysis, the higher the R^2 value (closer to unity), the better is the model for depicting the isotherm and kinetic model parameters. Apart from the correlation coefficient (R^2), the applicability and validity of isotherm and kinetic models for fitting the sorption data were evaluated by calculating the sum of squared errors (SSE), which can be expressed as:

$$\mathrm{SSE} = \sum \left(q_{e\mathrm{exp}} - q_{e\mathrm{cal}} \right)^2 / \left(q_{e\mathrm{exp}} \right)^2 \quad (9)$$

where $q_{e\mathrm{exp}}$ and $q_{e\mathrm{cal}}$ are the experimental fluoride adsorption capacity (mg/g) at equilibrium and the corresponding calculated value of adsorption capacity (mg/g) obtained from the respective models. It is assumed that the model which gives the lowest SSE values is the best model for a particular system. Thus, the isotherm and kinetic parameters were determined by minimizing the respective error function across the concentration range studied.

3. Results and discussion

3.1. Characterization of SBP

The performance of an adsorbent is highly influenced by its physical and chemical properties. The BET surface area and pore diameter of SBP was found to be 1.87 m^2/g and 16.1 Å, respectively. According to the International Union of Pure and Applied Chemistry, pores are classified on the basis of pore diameter as micropores ($dp < 20$ Å), mesopores (20 Å ≤ $dp < 500$ Å) and macropores ($dp \geq 500$ Å). In this case, the higher content of cellulose in the peels might have resulted in the formation of micropores. The specific surface area of SBP is similar to other fruit and vegetable peel based-adsorbents like pomegranate peel (1.28 m^2/g), pineapple peel (1 m^2/g), watermelon peel (1.44 m^2/g), garlic peel (1.40 m^2/g), green pea peel (1.02 m^2/g) and pigeon pea peel (1.04 m^2/g) used for defluoridation [18]. The low surface area of SBP signifies its fibrous nature and presence of carbonaceous materials [19].

Adsorption is a surface phenomenon, so the surface morphology of adsorbent provides a better understanding of the adsorbent–fluoride interactions. Figs. 1(a) and (b) represent the SEM images of the SBP before and after fluoride adsorption at 500× magnification. From the micrographs, pore development and changes in the surface texture of adsorbents are clearly visible. Before adsorption, the adsorbent exhibited an irregular and rough porous surface with heterogeneous voids and plate-like structures. These structures act as reactive adsorption centers for fluoride. After the adsorption, SBP appears to have a dense smooth surface, as the pores and caves were partially covered by fluoride.

The FTIR spectra (Fig. 2) of the prepared adsorbent displays a number of peaks, indicating its complex nature. The broad absorption band at 3,424.5 cm^{-1} is assigned to the O–H stretching of hydroxyl groups of alcohols and phenols. The peaks pertaining to 2,919.3 cm^{-1} are due to C–H stretching of alkane and alkene representing the aliphatic nature of the adsorbent, while the sharp peak at 1,758.5 cm^{-1} appears because of the asymmetrical stretching of C–H and C=O bonds of carboxylic acids or esters. The peak at 1,368.4 cm^{-1} occurs from the O–H bending of H_2O molecules present in the peel. Peaks at 1,044.4 and 1,090.8 cm^{-1} are attributed to Si–O stretching and Si–O bending, which signify the presence of silica. The significant amount of oxygen containing groups is mainly from the carbohydrates and fibers in the banana peel. Moreover, peaks in the region of lower wave numbers are due to nitrogen containing bioligands and N–H deformation of amines [20,21].

Thus, SBP is mainly composed of polymers such as lignin, hemicellulose and pectins, which contain various rich organic functional groups (–OH, $–NH_2$, –COOH), playing a major role in fluoride removal. These groups are responsible for Van der Waals forces, interparticle bridging, hydrogen bonding, substitution and columbic interactions between the SBP and fluoride ions. The shifting of –OH and the slight decrease in intensity after fluoride adsorption indicate the involvement of carboxylic and hydroxyl groups in the fluoride adsorption [22].

It was also reported that potassium was the most significant mineral present in the cooking banana cultivar, followed by magnesium, calcium, iron, sodium and zinc [23]. Micronutrients (Fe and Zn) were reported to be found in a higher level in peels, compared with pulps. Calcium enriched adsorbents are reported to show good defluoridation activity, as they basically favor the adsorption of fluoride as calcium fluoride [24]. It can be inferred that the presence of a high amount of calcium can help in fluoride adsorption when using SBP as an adsorbent.

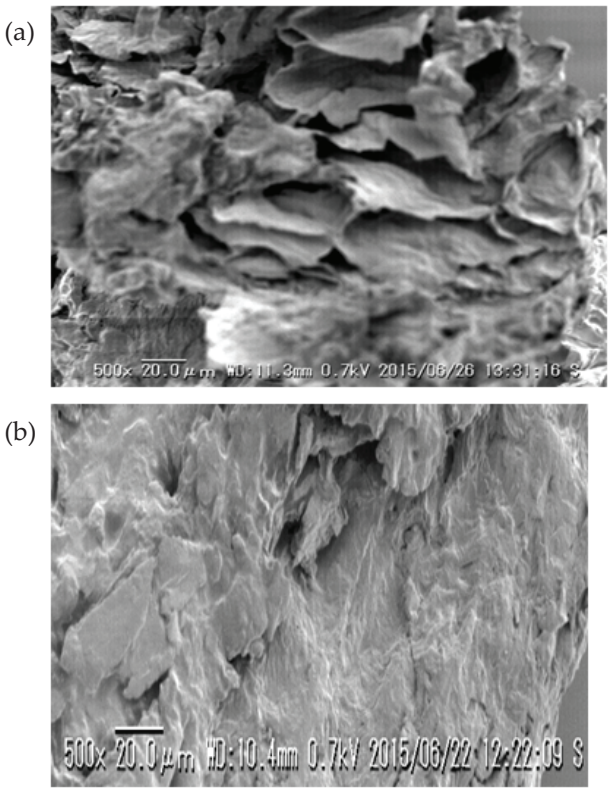

Fig. 1. SEM images for Saba banana peel (SBP): (a) before adsorption; (b) after fluoride adsorption.

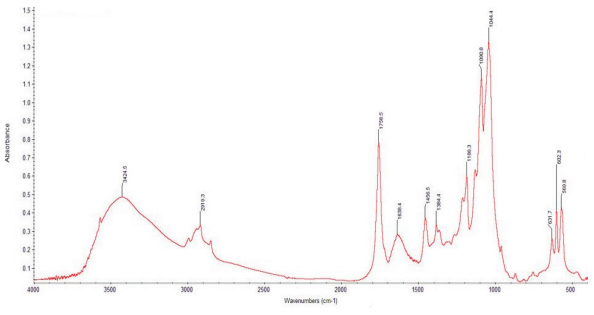

Fig. 2. FTIR spectra of Saba banana peel (SBP).

3.2. Optimization of reaction conditions

3.2.1. Optimization of adsorbent dose

The response of adsorbent dose on fluoride removal is presented in Figs. 3(a) and (b).

It is seen that the fluoride removal efficiency increased from 52% to 76% with the increment in SBP dose from 0.5 to 5 g/L. At higher doses of SBP, the availability of adsorption sites for fluoride ions is increased. At a lower dose, the amount of fluoride ions is relatively higher compared with adsorption sites, resulting in lower removal efficiency [25]. In contrast, there was a small increase in adsorption with an increase in SBP dosage. The adsorption capacity dropped from 10.4 mg/g at 0.5 g/L to 1.52 mg/g at 5 g/L dose. This is because of a lower adsorptive capacity utilization of adsorbent, termed as the 'solid concentration effect' [26]. Such aggregation would result in reduction of total surface area of adsorbent and the diffusional path length is increased.

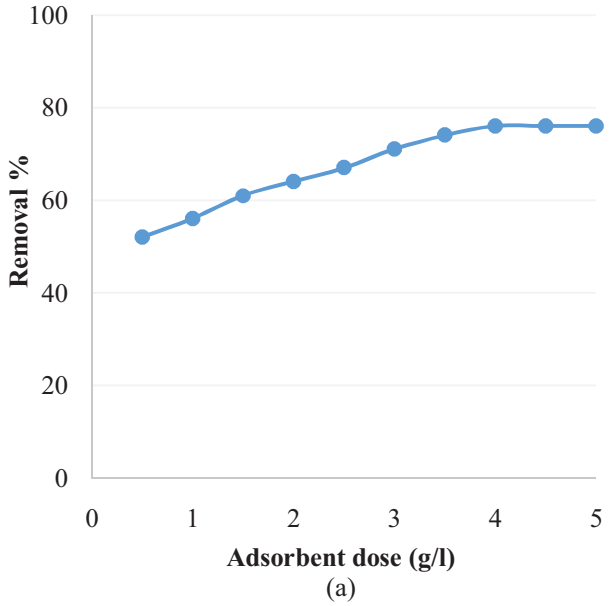

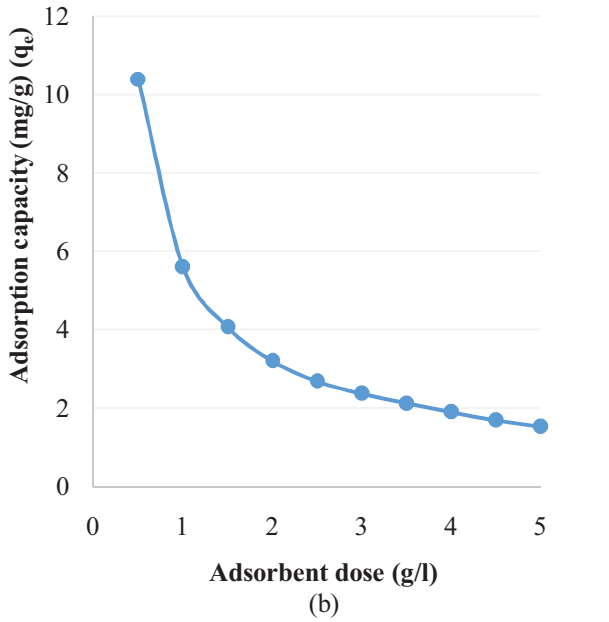

Fig. 3. (a) Effect of adsorbent dose on the percentage removal of fluoride by SBP, and (b) effect of adsorbent dose on the adsorption capacity of SBP (initial fluoride concentration: 10 mg/L, pH: 7, agitation speed: 150 rpm, contact time: 2 h).

Since SBP is an eco-friendly adsorbent without any negative health impacts, 4 g/L is chosen as a suitable dose at which 76% removal efficiency was recorded.

3.2.2. Optimization of pH value

As seen from Fig. 4(a), the removal efficiency increased from acidic to neutral pH, and then decreased slowly with further increase in pH. A maximum removal efficiency (76%) was observed at neutral pH. The SBP worked very well in the acidic and neutral pH range, probably due to strong columbic attraction between negatively charged F^- ions and positively charged H^+ ions on the adsorbent surface. In acidic medium, the surface functional groups on SBP exert positive charge, resulting in the sorption of fluoride. However, at extremely low pH, formation of weakly ionized hydrofluoric acid (pKa = 3.2) decreased fluoride adsorption. In alkaline medium, the increased concentration of hydroxyl ions hindered the diffusion of fluoride ions onto the porous sites, resulting in lower removal efficiency. Also, the formation of aqua complexes leads to desorption of fluoride ions at basic pH. Similar findings were reported using the active carbon derived from barks of *Vitex negundo* plant and *Polyalthia longifolia* leaf powder for fluoride removal [7,27].

This result can be also be discussed on the basis of the pH_{PZC} value of SBP (6.9), calculated from Fig. 4(b). An understanding of pH_{PZC} is useful to hypothesize the ionization of functional groups present in adsorbents and their interaction with ionic species in solution. As seen from Figs. 4(a) and (b), fluoride removal is favorable when the pH of solution is lower than the pH_{PZC} of adsorbents ($pH < pH_{PZC}$). High removal efficiency at neutral pH demonstrates the practical applicability of SBP.

The following reactions explain the fluoride adsorption behavior by lignocellulosic adsorbents like SBP under different pH values [28]:

$$\left.\begin{aligned} -SOH + H^+ &\leftrightarrow -SOH_2^+ \\ -SOH_2^+ + F^- &\leftrightarrow -SF + H_2O \end{aligned}\right\} \text{Two - step ligand exchange}$$

$$-SOH + F^- \leftrightarrow -SF + OH^-$$

$$-SOH + OH^- \leftrightarrow SO^- + H_2O$$

where, –SOH, $-SOH_2^+$ and SO^- are the neutral, protonated and deprotonated sites on SBP, and –SF is the active site–fluoride complex (S = adsorbent surface).

3.2.3. Optimization of agitation speed

The obtained results were plotted as removal percentage of fluoride vs. agitation speed, as shown in Fig. 5. It is seen that the rate of removal increases with agitation speed and reaches a maximum of 83% at 300 rpm. The increase in

removal efficiency with agitation speed confirms the influence of external diffusion on sorption kinetics [29]. The proper contact between the F^- ion in solution and binding sites at higher speed promoted the effective transfer of fluoride ions onto the SBP sites. At lower speeds, the adsorbent accumulated at the flask bottom, resulting in the burial of active sites. The presence of liquid film thickness around the particles also decreases the uptake rate [30]. However, it should be considered that random spreading of adsorbent particles at high speeds may not allow sufficient time for binding the fluoride ions.

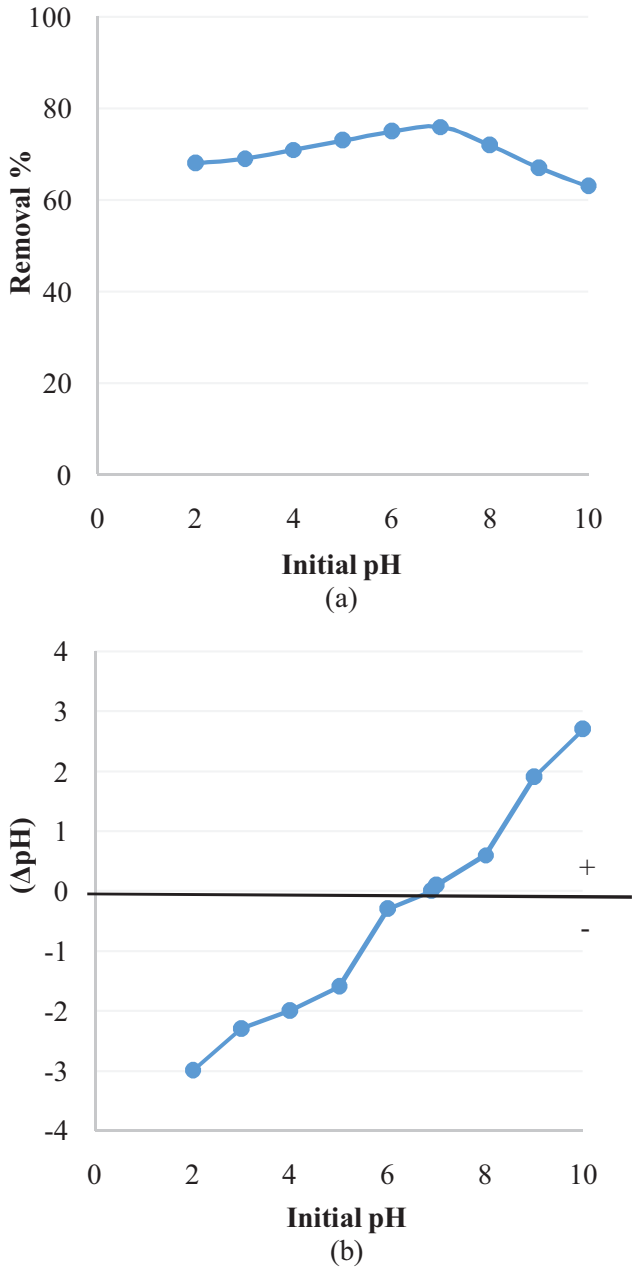

Fig. 4. (a) Effect of pH on the removal of fluoride by SBP (initial fluoride concentration: 10 mg/L, adsorbent dose: 4 g/L, agitation speed: 150 rpm, contact time: 2 h). (b) Estimation of point of zero charge (pH_{PZC}) of SBP at 35°C.

A speed of 200 rpm is sufficient to ensure that all the binding sites equally interacted with fluoride ions.

3.2.4. Optimization of contact time

The contact time curve in Fig. 6 shows that the fluoride removal efficiency of SBP increased with the duration of its exposure to fluoridated water. Instantaneous sorption was noticed in the initial stage as a result of specific chemical interactions or other driving forces like diffusion. The curve became flat after 160 min, denoting the attainment of equilibrium. There was no significant uptake after this point due to a decrease in fluoride concentration in the solution and limitations of binding sites in SBP for coordination of fluoride ions [31].

3.2.5. Effect of initial fluoride concentration

The effect of initial fluoride concentration on the fluoride removal can be clearly understood from Fig. 7. The results indicate that the removal was maximum at 5 mg/L concentration, which decreased continuously to 52% for 40 mg/L F^-. This is because at low concentrations, there is an active interaction of fluoride ions with the available binding sites, facilitating higher removal efficiency. As the ratio of fluoride ions to SBP increases at higher concentrations, this results in faster saturation of higher energy sites. The fluoride ions compete for remaining low energy sorption sites, causing a decrease in removal efficiency [32].

Conversely, the main driving force for transportation of fluoride from the bulk to the adsorbent surface increases with increasing concentration. This results in more fluoride adsorption per unit mass of the SBP (mg/g), as seen from Fig. 7(b).

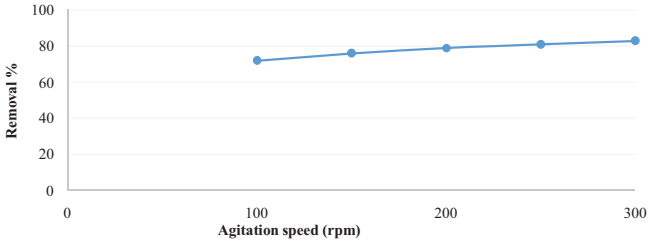

Fig. 5. Effect of agitation speed on the removal of fluoride by SBP (initial fluoride concentration: 10 mg/L, adsorbent dose: 4 g/L, pH: 7, contact time: 2 h).

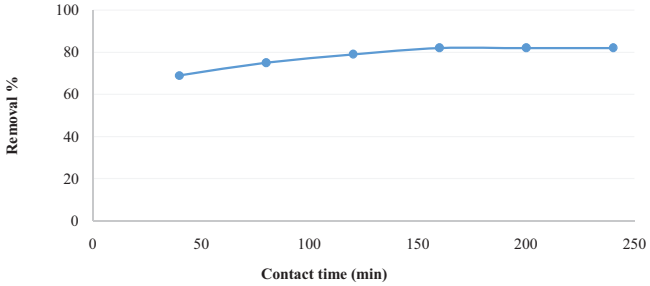

Fig. 6. Effect of contact time on the removal of fluoride by SBP (initial fluoride concentration: 10 mg/L, adsorbent dose: 4 g/L, pH: 7, agitation speed: 200 rpm).

3.2.6. Effect of co-existing ions

It can be inferred from Fig. 8 that there was no significant effect on fluoride removal in the presence of monovalent chloride ions, while the presence of divalent sulfate at higher concentrations resulted in a decrease of fluoride removal efficiency. The fluoride removal efficiency reduced from 79% to 77% and 75% to 68% on increasing the chloride and sulfate concentration from 50 to 250 mg/L, respectively. This is because chloride ion is a low-affinity ligand, and its adsorption mechanism is via formation of weaker bonds with active sites at outer-sphere complexation. Hence, fluoride ions are adsorbed through the formation of strong bonds with accessible binding sites at inner-sphere complexation. Sulfate ions, on the other hand, partially form inner- and outer-sphere complexes [33,34]. Besides, there may be competition between fluoride and sulfate ions for the sorption sites, as high columbic repulsion may reduce the interaction of fluoride with the binding sites.

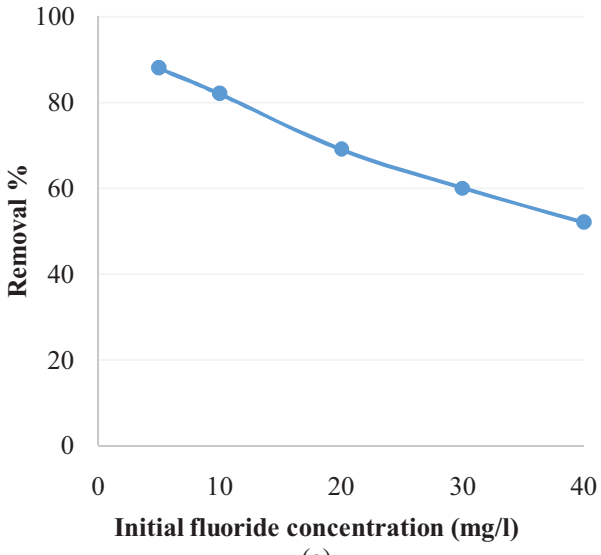

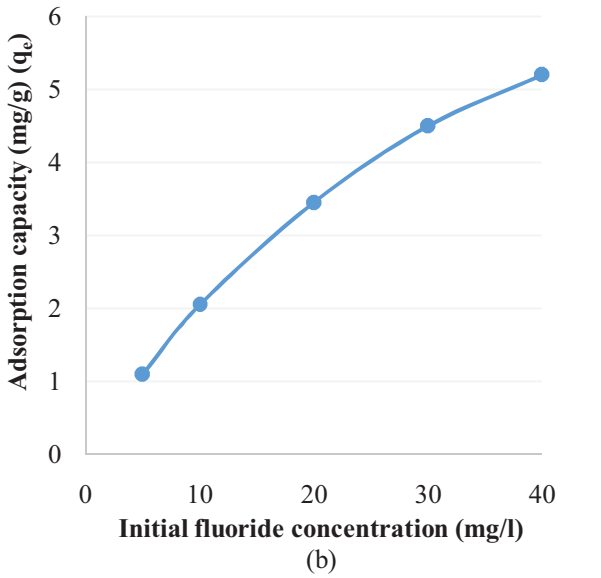

Fig. 7. Effect of initial fluoride concentration on the removal of fluoride by SBP (adsorbent dose: 4 g/L, pH: 7, agitation speed: 200 rpm, contact time: 160 min).

3.3. Adsorption isotherm studies

The equilibrium isotherms for the adsorption of fluoride onto SBP at pH 7 and 298 K are shown graphically in Figs. 9 and 10. The plot of separation factor (R_L) values and initial fluoride concentrations (C_i) in Fig. 10 explains the crucial features of the Langmuir isotherm. The isotherm parameters obtained from the slope and intercept values of the respective plots, and the calculated SSE values are given in Table 1.

The R^2 values of both isotherms approach to one, which denote a linear relationship and emphasize the probability of mono and heterolayer formation on the SBP surface. A steep initial slope, that is, a higher value of '*b*' signifies the existence of stronger bonds between fluoride and SBP, and revalidates that one of the dominant modes of adsorption is chemisorption. Moreover, the Freundlich isotherm provided a concise analytical expression for the experimental facts. The magnitudes of K_F and n indicated easy removal of fluoride ions and verified that the adsorption process is favorable. The surface becomes more heterogeneous as the '1/*n*' value approaches zero. In this study, the value of 1/*n* is less than one, implying the involvement of chemisorption process in fluoride removal [12].

The calculated values of the separation factor, R_L, for SBP were found to be 0.414, 0.261, 0.150, 0.105 and 0.081 for 5, 10, 20, 30 and 40 mg/L fluoride concentrations, respectively. This indicates that the fluoride adsorption by SBP was favorable under optimum conditions. Moreover, a steeper isotherm in Fig. 10 suggests that the tested adsorbent is highly effective for fluoride removal.

3.4. Adsorption kinetic studies

Adsorption kinetics describes the fluoride removal rate with respect to equilibrium contact time. The linear analysis of adsorption data with three different kinetic models is shown graphically in Fig. 11. The values of the respective plots and the calculated SSE values for the tested models are listed in Table 2.

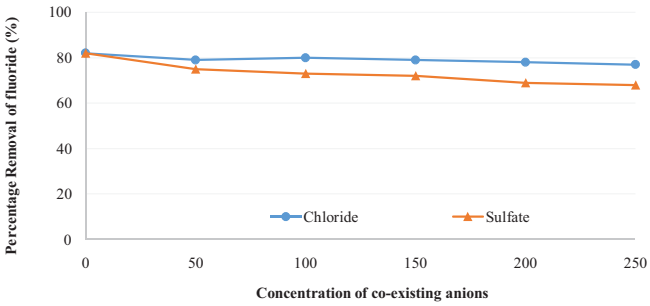

Fig. 8. Effect of co-existing anions on the removal of fluoride by SBP (fluoride concentration: 10 mg/L, adsorbent dose: 4 g/L, pH: 7, agitation speed: 200 rpm, contact time: 160 min).

As seen from Fig. 11, even though the intraparticle diffusion plots are linear, they fail to pass through the origin. This variation from the origin may be because of the difference of mass transfer in the initial and final stages of adsorption [35]. In such cases, adsorption kinetics of fluoride is controlled by both surface adsorption and intraparticle diffusion, simultaneously. The multi-linear plots in Fig. 11(a), concludes that the sorption process is 'complex', including more than one mechanism.

The equilibrium data is represented well by the pseudo-first-order model only in the initial stage where the

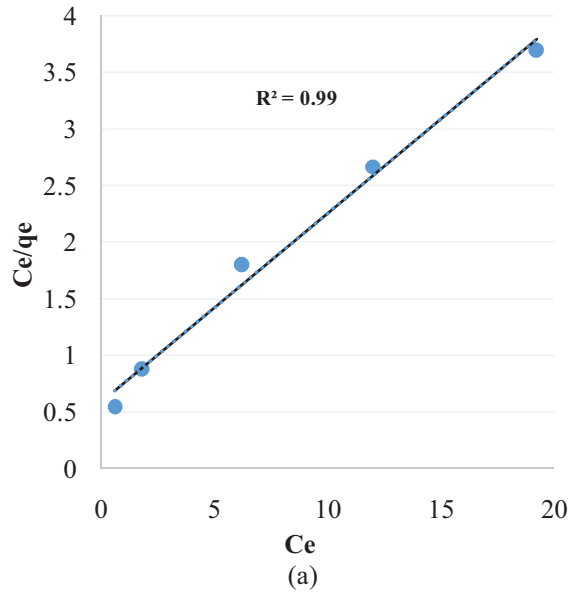

Fig. 9. (a) Langmuir isotherm model and (b) Freundlich isotherm model for adsorption of fluoride onto SBP (adsorbent dose: 4 g/L, pH: 7, temperature: 298 K, agitation speed: 200 rpm, contact time: 160 min).

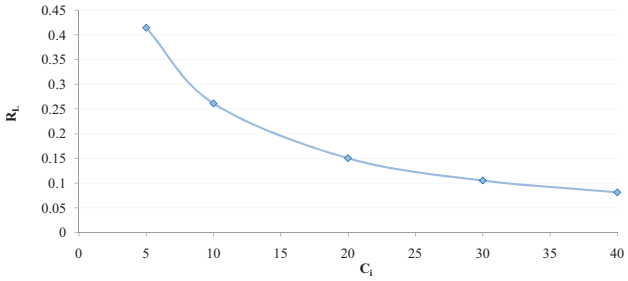

Fig. 10. Separation factor R_L values vs. initial fluoride concentration (C_i).

Table 1
Calculated parameters and SSE values of Langmuir and Freundlich isotherm models at pH 7 and 298 K

Isotherm	Parameters				
Langmuir isotherm	R^2	Q_o	b	SSE	
	0.990	5.9	0.283	0.012	
Freundlich isotherm	R^2	K	n	$1/n$	SSE
	0.991	1.46	2.23	0.44	0.010

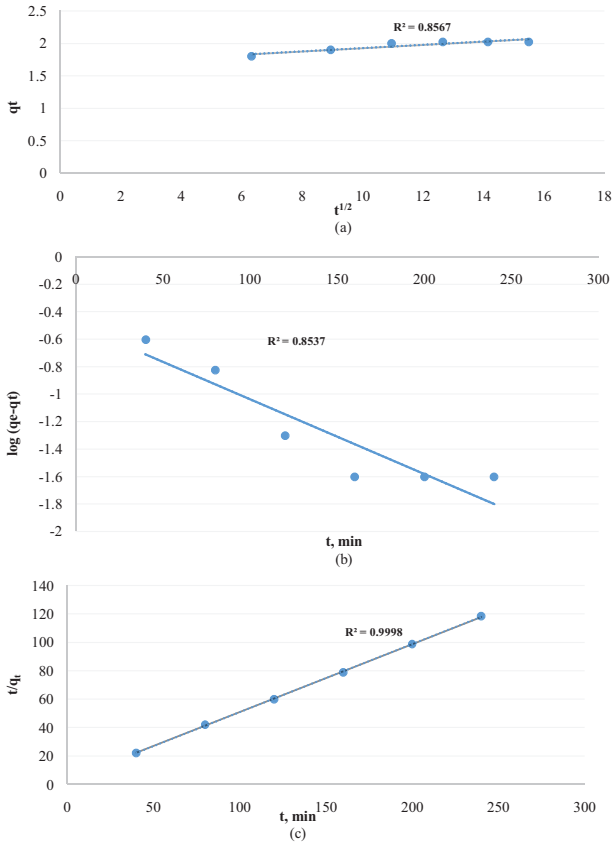

Fig. 11. (a) Intraparticle diffusion model, (b) pseudo-first-order kinetic model and (c) pseudo-second-order kinetic model for adsorption of fluoride onto SBP (initial fluoride concentration: 10 mg/L, adsorbent dose: 4 g/L, pH: 7, temperature: 298 K, agitation speed: 200 rpm).

adsorption rate of fluoride is very rapid. A trial and error method is used to find the equilibrium adsorption capacity, q_e, to understand the applicability of this model.

Similarly, a straight line fit with high correlation coefficient shows that the experimental data was well represented by the pseudo-second-order kinetic model. For these types of reactions, the rate of adsorption is directly proportional to the number of active sites on the adsorbent surface.

The correlation coefficient (R^2) values for all three models were found to follow the order: pseudo-second-order model > intraparticle diffusion model > pseudo-first-order model. Thus, the pseudo-second-order model provides the best fit to the experimental data, and the overall rate of fluoride adsorption seems to be controlled by the chemical process. So, the adsorption of F^- by SBP is an irreversible process, and its main drawback is associated with the regeneration of adsorbent. Finding proper techniques for the regeneration of adsorbent is therefore critical to performance enhancement and reusability. Low correlation coefficient values for the first-order kinetic model indicate that the adsorption of fluoride does not occur exclusively as one site per ion. Also, the experimental and calculated values of adsorption capacity did not agree with each other. So, this model did not fit the complete range of contact time and is relevant only for the early stage of the process. A higher value of '*C*' for the intraparticle diffusion model signifies a higher boundary layer effect, and there is greater importance of surface adsorption in the rate determining step [36]. Further, lower values of SSE for the pseudo-second-order model showed a better fit to the sorption data and gave an indication of the sorption mechanism.

Table 2
Calculated Parameters and SSE values of the selected kinetic models at pH 7 and 298 K

Isotherm	Parameters					
Intra-particle diffusion model	R^2	k_{int}	C		SSE	
	0.856	0.025	1.672		0.0098	
Pseudo-first-order model	R^2	K_1	$q_e$cal	$q_e$exp	SSE	
	0.853	0.012	0.322	2.05	0.7105	
Pseudo-second-order model	R^2	K_2	$q_e$cal	$q_e$exp	h	SSE
	0.999	0.075	2.088	2.05	0.327	0.000034

3.5. Comparison with other adsorbents

The defluoridation capacity of Saba banana peel has been compared with those of other adsorbents reported in the literature (Table 3). It can be seen that this adsorbent has a higher adsorption capacity than several other plant-based adsorbents, indicating its potential in treating fluoride contaminated water due to its relative abundance and convenient reaction conditions.

4. Conclusions

This study shows the potential of employing easily available and inexpensive Saba banana peel for the treatment of fluoride contaminated water. It showed relatively high adsorption capacity than several plant-based adsorbents. The removal efficiency of the banana peel powder was found to increase with increasing dose of biomass and exposure time, with constant agitation speed (200 rpm), whereas the removal rate decreased with an increase in initial fluoride concentration. At low fluoride concentration, the adsorbent exhibited high selectivity for fluoride ions with co-existing chloride and sulfate ions in a binary system. The main advantage of using this agro-based adsorbent is that it works optimally at pH 6 and 7, which reduces the cost of

Table 3
Comparison of the adsorption capacities of different adsorbents for defluoridation at various operating conditions

Adsorbents	Optimum pH	Optimum dose (g/L)	Contact time (min)	Adsorption capacity (mg/g)	Ref.
Pumice functionalized by hexadecyltrimethyl ammonium (HDTMA)	6	0.5	30	41	[37]
Ferric-stilbite zeolite	6.94	10	120	2.31	[38]
Treated coffee husk	2	18	180	0.4159	[10]
Treated banana (*Musa paradisiaca*) peel	2	24	780	0.3950	
Treated leaf biomass (crude fiber content from neem, pipal and khair)	2	10	90	0.04	[39]
Seeds of cabbage tree (*Moringa stenopetala*)	7	2	60	1.32	[5]
Zirconium impregnated lapsi seed stone activated carbon	3–4	2	180	3.25 mg/g at pH 3 1.6 mg/g at pH 7	[40]
Neem *(Azadirachta indica*) stem charcoal	5	5	180	1.27	[32]
Activated stalks of Sorghum (*Sorghum bicolor*)	5	10	60	7.8	[6]
Activated stalks of Canola (*Brassica napus*)	5	10	90	8.24	
Saba banana peel	7	4	160	5.99	This study

post defluoridation pH adjustment. When the initial fluoride concentration is maintained at 5 mg/L, the removal efficiency of the adsorbent is 88% at optimum conditions, and fluoride concentration of the treated water meets the standard. Naturally dispersed calcium ions in SBP could have helped in the adsorption of negatively charged fluoride ions. The availability of highly active surface functional groups like (–OH, $–NH_2$, –COOH) in SBP played more of a role in process efficiency than the specific surface area. It is beneficial to enhance the population of these functional groups on the adsorbent surface through acid treatment or quaternization (surface chemical treatment) for better performance. Both Langmuir and Freundlich isotherm models fitted well to the experimental data and are statistically significant. Adsorption of fluoride followed the second-order reaction model, and the mechanism of fluoride removal on adsorbents was found to be complex with the involvement of more than one step. Finally, banana peel powder can be employed as an eco-friendly and cost-effective adsorbent for the defluoridation of water.

Since this non-conventional adsorbent is available abundantly, there is no need to regenerate the exhausted peel powder. It can be used once and dumped as a filler material in low-lying areas without changing the chemical nature of soil because the adsorbent works at neutral pH.

Symbols

C_i	—	Liquid-phase fluoride concentrations at initial time, mg/L
C_e	—	Liquid-phase fluoride concentrations at equilibrium time, mg/L
W	—	Dry weight of the adsorbent, g
V	—	Volume of fluoride solution, L
q_e	—	Amount of fluoride adsorbed per unit weight of adsorbent at equilibrium, mg/g
q_t	—	Amount of fluoride adsorbed per unit weight of adsorbent at time t (min), mg/g
Q_o	—	Langmuir constant related to the maximum adsorption capacity, mg/g
b	—	Langmuir constant related to the adsorption affinity coefficient, L/mg
R_L	—	Separation factor representing the essential features of Langmuir isotherm
K	—	Freundlich constant denoting the adsorption capacity, mg/g
n	—	Freundlich constant denoting the adsorption intensity
K_1	—	Pseudo-first-order rate constant, min^{-1}
K_2	—	Pseudo-second-order rate constant, g mg^{-1} min^{-1}
h	—	Initial adsorption rate of fluoride, mg g^{-1} min^{-1}
k_{int}	—	Intraparticle diffusion coefficient, mg g^{-1} $min^{-0.5}$
C	—	Intraparticle diffusion constant, related to the boundary layer thickness, mg g^{-1}
q_{eexp}	—	Experimental fluoride adsorption capacity at equilibrium, mg/g
q_{ecal}	—	Calculated values of fluoride adsorption capacity obtained from the respective kinetic models, mg/g

References

[1] R. Soni, S. Modi, A review on effects of fluoride on human health in Rajasthan, Int. J. Innovative Res. Dev., 2 (2013) 638–646.

[2] M. Sutton, R. Kiersey, L. Farragher, J. Long, Health Effects of Water Fluoridation, Health Research Board, Dublin, Ireland, 2015.

[3] N.A. Ingle, H.V. Dubey, N. Kaur, I. Sharma, Defluoridation techniques: which one to choose, J. Health Res. Rev., 1 (2014) 1–4.

[4] S.S. Waghmare, T. Arfin, Fluoride removal from water by various techniques: review, Int. J. Innovative Sci. Eng. Technol., 2 (2015) 560–571.

[5] S.T. Mereta, Biosorption of fluoride ion from water using the seeds of the cabbage tree (*Moringa stenopetala*), Afr. J. Environ. Sci. Technol., 11 (2017) 1–10.

[6] M.A. Zazouli, A.H. Mahvi, Y. Mahdavi, D. Balarak, S. Tehran, Z. Iran, Isothermic and kinetic modeling of fluoride removal from water by means of the natural biosorbents sorghum and canola, Fluoride, 48 (2015) 37–44.

[7] M. Suneetha, B.S. Sundar, K. Ravindhranath, Removal of fluoride from polluted waters using active carbon derived from barks of *Vitex negundo* plant, J. Anal. Sci. Technol., 6 (2015) 1–19.

[8] N. Gandhi, D. Sirisha, K.B. Chandra Shekar, S. Asthana, Removal of fluoride from water and waste water by using low cost adsorbents, Int. J. ChemTech Res., 4 (2012) 1646–1653.

[9] D.D. Pandey, A. Tripathi, T.P. Singh, Removal of flouride from industrial waste water using Mosambi peel as biosorbent: kinetics studies, Int. J. Sci. Eng. Technol., 4 (2016) 72–81.

[10] T. Getachew, A. Hussen, V.M. Rao, Defluoridation of water by activated carbon prepared from banana (*Musa paradisiaca*) peel and coffee (*Coffea arabica*) husk, Int. J. Sci. Eng. Technol., 12 (2015) 1857–1866.

[11] S.P. Kapadia, P.S. Pudakalkatti, S. Shivanaikar, Detection of antimicrobial activity of banana peel (*Musa paradisiaca* L.) on *Porphyromonas gingivalis* and *Aggregatibacter actinomycetemcomitans*: an in vitro study, Contemp. Clin. Dent., 6 (2015) 496–499.

[12] K.Y. Foo, B.H. Hameed, Insights into the modeling of adsorption isotherm systems, Chem. Eng. J., 156 (2010) 2–10.

[13] G. Alagamuthu, V. Veeraputhiran, R. Venkataraman, Fluoride sorption using *Cynodon dactylon* based activated carbon, Hemijska Industrija, 65 (2011) 23–25.

[14] L. Liu, J. Liu, H. Li, H. Zhang, J. Liu, H. Zhang, Equilibrium, kinetic, and thermodynamic studies of lead (II) biosorption on sesame leaf, BioResources, 3 (2012) 3555–3572.

[15] N.P. Kumar, N.S. Kumar, A. Krishnaiah, Defluoridation of water using Tamarind (*Tamarindus indica*) fruit cover: kinetics and equilibrium studies, J. Chil. Chem. Soc., 57 (2012) 1224–1231.

[16] G. Vijayakumar, R. Tamilarasan, M. Dharmendirakumar, Adsorption, kinetic, equilibrium and thermodynamic studies on the removal of basic dye Rhodamine-B from aqueous solution by the use of natural adsorbent perlite, J. Mater. Environ. Sci., 3 (2012) 157–170.

[17] C.H. Yang, M.C. Shih, H.C. Chiu, K.S. Huang, Magnetic *Pycnoporus sanguineus*-loaded alginate composite beads for removing dye from aqueous solutions, Molecules, 19 (2014) 8276–8288.

[18] P.D. Pathak, S.A. Mandavgane, B.D. Kulkarni, Characterizing fruit and vegetable peels as bioadsorbents, Current Sci., 110 (2016) 2114–2123.

[19] R.S.D. Castro, L. Caetano, G. Ferreira, P.M. Padilha, M.J. Saeki, L.F. Zara, M.A.U. Martines, G.R. Castro, Banana peel applied to the solid phase extraction of copper and lead from river water: preconcentration of metal ions with a fruit waste, Ind. Eng. Chem. Res., 50 (2011) 3446–3451.

[20] J.R. Memon, S.Q. Memon, M.I. Bhanger, M.Y. Khuhawar, Banana peel: a green and economical sorbent for Cr (III) removal, Pak. J. Anal. Environ. Chem., 9 (2008) 20–25.

[21] M.S. Mahmoud, S.M. Ahmed, S.G. Mohammad, A.M.A. Elmagd, Evaluation of Egyptian banana peel (*Musa* sp.) as a green sorbent for groundwater treatment, Int. J. Eng. Technol., 4 (2014) 648–659.

[22] N.K. Mondal, Natural banana (*Musa acuminate*) peel: an unconventional adsorbent for removal of fluoride from aqueous solution through batch study, Water Conserv. Sci. Eng., 1 (2017) 223–232.
[23] G.A. Annor, P. Asamoah-Bonti, E. Sakyi-Dawson, Fruit physical characteristics, proximate, mineral and starch characterization of FHIA 19 and FHIA 20 plantain and FHIA 03 cooking banana hybrids, SpringerPlus, 5 (2016) 796.
[24] R. Shyam, G.S. Kalwania, Accumulation of fluoride in sikar aquifer and their removal by khimp powder, Orient. J. Chem., 29 (2013) 1169–1177.
[25] P.S.P. Harikumar, C. Jaseela, T. Megha, Defluoridation of water using biosorbents, Nat. Sci., 4 (2012) 245–251.
[26] N. Gupta, V. Gupta, A.P. Singh, R.P. Singh, Defluoridation of groundwater using low cost adsorbent like bagasse dust, aluminium treated bagasse flyash, bone powder and shell powder, Bonfring Int. J. Ind. Eng. Manage. Sci., 4 (2014) 72–75.
[27] R.K. Bharali, K.G. Bhattacharyya, Kinetic and thermodynamic studies on fluoride biosorption by Devdaru (*Polyalthia longifolia*) leaf powder, Octa J. Environ. Res., 2 (2014) 22–31.
[28] A.A.M. Daifullah, S.M. Yakout, S.A. Elreefy, Adsorption of fluoride in aqueous solutions using $KMnO_4$– modified activated carbon derived from steam pyrolysis of rice straw, J. Hazard. Mater., 147 (2007) 633–643.
[29] M.M.A. El-Latif, A.M. Ibrahim, M.F. El-Kady, Adsorption equilibrium, kinetics and thermodynamics of methylene blue from aqueous solutions using biopolymer oak sawdust composite, J. Am. Sci., 6 (2010) 267–283.
[30] J. Anwar, U. Shafique, W.U. Zaman, M. Salman, A. Dar, S. Anwar, Removal of Pb (II) and Cd (II) from water by adsorption on peels of banana, Bioresour. Technol., 101 (2010) 1752–1755.
[31] S. Koshle, S. Mahesh, S.N. Swamy, Isolation and identification of *Trichoderma harzianum* from groundwater: an effective biosorbent for defluoridation of groundwater, J. Environ. Biol., 37 (2016) 135–140.
[32] S. Chakrabarty, H.P. Sharma, Defluoridation of contaminated drinking water using neem charcoal adsorbent: kinetics and equilibrium studies, Int. J. ChemTech Res., 4 (2012) 511–516.
[33] L. Liu, Z. Cui, Q. Ma, W. Cui, X. Zhang, One-step synthesis of magnetic iron–aluminum oxide/graphene oxide nanoparticles as a selective adsorbent for fluoride removal from aqueous solution, RSC Adv., 6 (2016) 10783–10791.
[34] S. Rajkumar, S. Murugesh, V. Sivasankar, A. Darchen, T.A.M. Msagati, T. Chaabane, Low-cost fluoride adsorbents prepared from a renewable biowaste: syntheses, characterization and modeling studies, Arabian J. Chem., (2015) https://doi.org/10.1016/j.arabjc.2015.06.028.
[35] C.H. Chakrapani, C.H.S. Babu, K.N.K. Vani, K.S. Rao, Adsorption kinetics for the removal of fluoride from aqueous solution by activated carbon adsorbents derived from the peels of selected citrus fruits, J. Chem., 7 (2010) 419–427.
[36] P. Satish, R. Sameer, P. Naseema, Defluoridation of water using biosorbents: kinetic and thermodynamic study, Int. J. Res. Chem. Environ., 3 (2013) 125–135.
[37] G. Asgari, B. Roshani, G. Ghanizadeh, The investigation of kinetic and isotherm of fluoride adsorption onto functionalize pumice stone, J. Hazard. Mater., 217 (2012) 123–132.
[38] Y. Sun, Q. Fang, J. Dong, X. Cheng, J. Xu, Removal of fluoride from drinking water by natural stilbite zeolite modified with Fe (III), Desalination, 277 (2011) 121–127.
[39] A.V. Jamode, V.S. Sapkal, V.S. Jamode, Defluoridation of water using inexpensive adsorbents, J. Indian Inst. Sci., 84 (2004) 163–171.
[40] S. Joshi, M. Adhikari, R.R. Pradhananga, Adsorption of fluoride ion onto zirconyl-impregnated activated carbon prepared from lapsi seed stone, J. Nepal Chem. Soc., 30 (2013) 13–23.